UNCLASSIFIED

NRL Report 6336

Principles and Instrumentation for the Measurement of Work-Function Variations by Electron-Beam Scanning

R. E. Thomas, G. A. Haas, and F. H. Harris

Electron Tubes Branch
Electronics Division

December 16, 1965

U.S. NAVAL RESEARCH LABORATORY
Washington, D.C.

UNCLASSIFIED

CONTENTS

Abstract	ii
Problem Status	ii
Authorization	ii
INTRODUCTION	1
PRINCIPLES OF MEASUREMENT	1
EXPERIMENTAL TUBE	5
DISPLAY SYSTEM	6
METHODS OF OBTAINING PATCH DISTRIBUTION	7
MEASUREMENT ERRORS AND LIMITATIONS	10
SUMMARY	13
REFERENCES	14

Copies available from Clearinghouse for Federal Scientific
and Technical Information (CFSTI) Sills Building,
5285 Port Royal Road, Springfield, Virginia 22151
$1.00

ABSTRACT

An experimental tube and associated circuitry have been developed to measure the point-by-point variation (or "patchiness") in the work function of conductive surfaces. The technique involves scanning the surface with a small-diameter, low-energy electron beam in a television-like fashion. An enlarged image showing the pattern of the work-function variation on the surface is obtained on a kinescope tube. The associated circuitry also provides a method of obtaining, during one scan, the values of the work functions of many small regions of the scanned surface. These individual values are automatically catalogued and stored by means of a 400-channel analyzer which gives a plot of the area distribution in work function in about three seconds.

The minimum work-function "patch" size that can be resolved is determined approximately by the size of the electron beam (work-function variations with dimensions as small as three microns have been observed). In measuring "patch" distributions the system is capable of resolving differences in work function as small as 0.025 ev. This instrumentation was primarily designed for the purpose of measuring patch distributions on surfaces that might be used as thermionic sources of electrons in vacuum tubes and energy converters. However, since measurements may be made over a wide range of surface temperatures, other surface phenomena, e.g., adsorption and surface migration, may also be studied using this equipment.

PROBLEM STATUS

This is an interim report on one phase of the problem; work on this and other phases is continuing.

AUTHORIZATION

NRL Problem R08-05
Project RR 008-03-46-5652

Manuscript submitted August 2, 1965.

PRINCIPLES AND INSTRUMENTATION FOR THE MEASUREMENT OF WORK-FUNCTION VARIATIONS BY ELECTROM-BEAM SCANNING

INTRODUCTION

Except for thoroughly "cleaned" single crystals, most surfaces do not have the same work function (w.f.) at every point, but are composed of areas that can differ in w.f. by as much as two or even three volts. The electron-beam scanning (E.B.S.) technique has been developed to provide a means of observing and measuring these nonuniformities in the w.f. of a surface. There are several other techniques that may be used to investigate nonuniformities in w.f. The relative merits and limitations of these methods, as well as a brief description of the E.B.S. technique, have already been presented in an earlier publication (1). Since that time, two major changes have been incorporated in the E.B.S. equipment. These are (a) a substantial decrease in beam diameter, and (b) the ability to obtain a plot of the area distribution in w.f.* by making only a single scan of the surface with the electron beam. These changes were motivated by a desire to resolve smaller "patches" and also to decrease the interaction of the electron beam with the target. This report describes in greater detail the complete measuring system in its present form and the principles and limitations of the E.B.S. technique.

PRINCIPLES OF MEASUREMENT

The basic principle of the E.B.S. technique is very similar to the method used by Anderson (2) to measure the contact potential between two surfaces. However, in the E.B.S. method current measurements are taken in the "deep retarding" field region, and the surface being examined is probed point by point with a small-diameter electron beam instead of being flooded with a large beam. The schematic diagram of the experimental tube in Fig. 1 indicates the path the beam must travel to reach the target. Figure 2 illustrates an idealized potential profile through which the electron beam must pass in going from an area of w.f. ϕ_c on the cathode to an area of w.f. ϕ_{T_1} on the target. Usually the ϕ_c will be a space-charge barrier in front of the cathode; V_c is the external voltage applied between the Fermi levels E_{f_c} and E_{f_T} of the cathode and target respectively. The quantity $E_B = (\phi_c - V_c)$ is the energy that an electron leaving the cathode with zero kinetic energy has with respect to the Fermi level of the target. Obviously when $E_B = \phi_{T_1}$, all electrons leaving the cathode can cross the barrier ϕ_{T_1} (we are here neglecting any reflection coefficient at the target). As E_B is made less than ϕ_{T_1}, some of the electrons in the beam are turned back, and the beam energy is in the "retarding field region." If the electrons that passed over the barrier had the ideal half-Maxwellian distribution of normal velocities,† and if no fields were encountered enroute to the target to perturb the normal velocity distribution, the current I vs E_B curve for electrons incident on an area of w.f. ϕ_{T_1} would follow the relation,

$$I = \begin{cases} I_m \exp\left[\dfrac{E_B - \phi_{T_1}}{kT_c}\right], & \text{for} \quad E_B < \phi_{T_1} \\ I_m, & \text{for} \quad E_B \geq \phi_{T_1} \end{cases} \tag{1}$$

*The area distribution in w.f. is defined as the fraction of the surface area having w.f. between ϕ and $\phi + \Delta\phi$ per unit range $\Delta\phi$.

†The normal velocity distribution is the distribution in velocities averaged over all velocities in the plane normal to the direction of the net current flow.

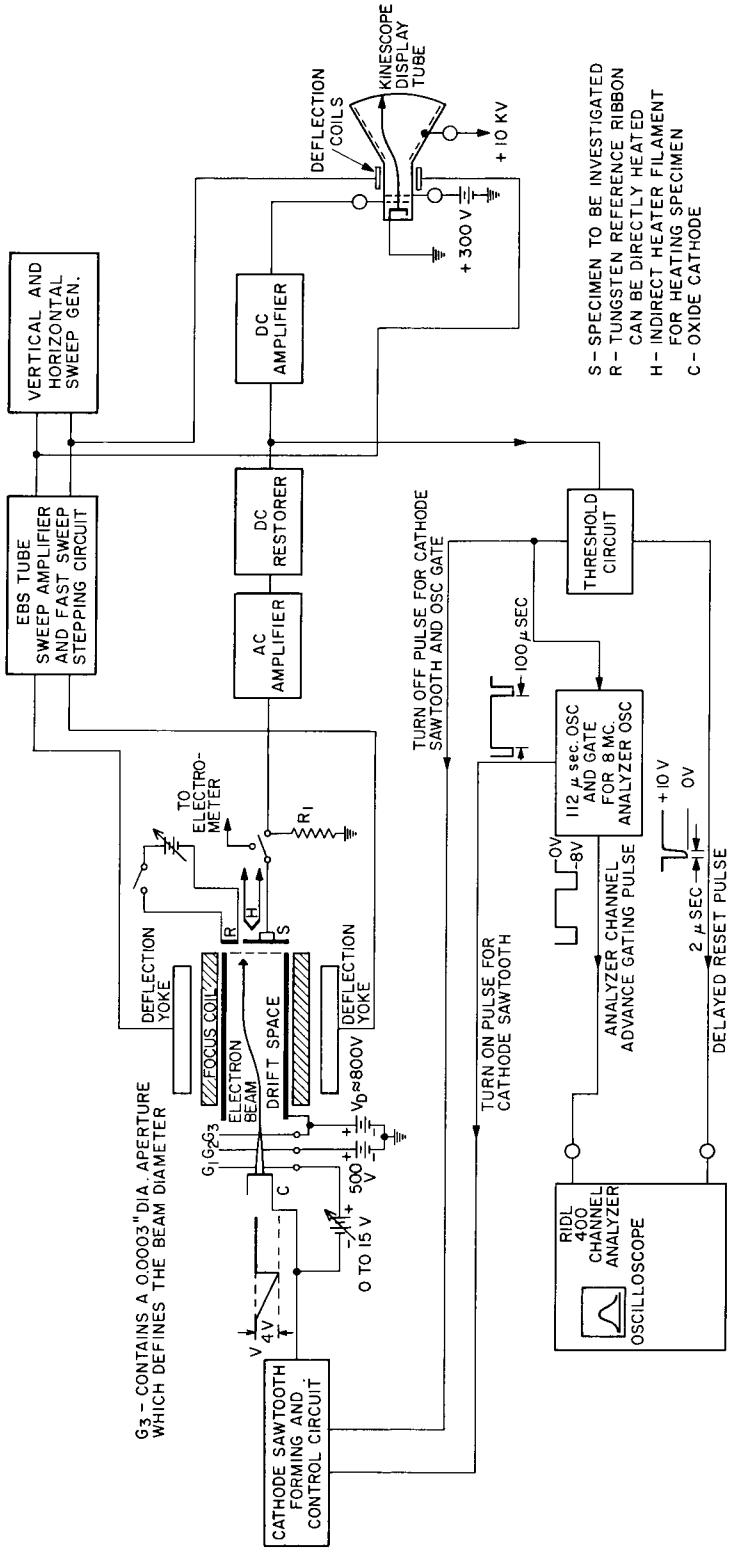

Fig. 1 - Schematic of electron-beam scanning tube and associated circuitry

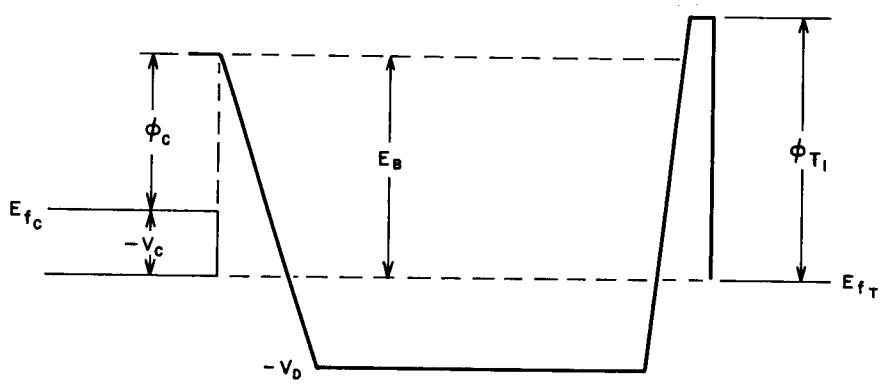

Fig. 2 - Idealized potential profile over the electron-beam path in the electron-beam scanning tube

in which k is Boltzmann's constant and T_c is the temperature of the cathode (°K). Figure 3 shows the I vs E_B curves that would be obtained from Eq. (1) for two areas having w.f.'s ϕ_{T_1} and ϕ_{T_2}. The curve for the area having w.f. ϕ_{T_2} would follow the dotted line of Fig. 3, if $\phi_{T_2} > \phi_{T_1}$. From the above definitions,

$$\phi_{T_2} - \phi_{T_1} = E_{B_2} - E_{B_1} = V_{C_2} - V_{C_1},$$

where V_{C_2} and V_{C_1} are the values of cathode voltage required to give the same current, say I_{th}. On these ideal curves I_{th} can be any value of current less than I_m. Unfortunately the retarding-field curves obtained in practice are not as predictable as those of Fig. 3.

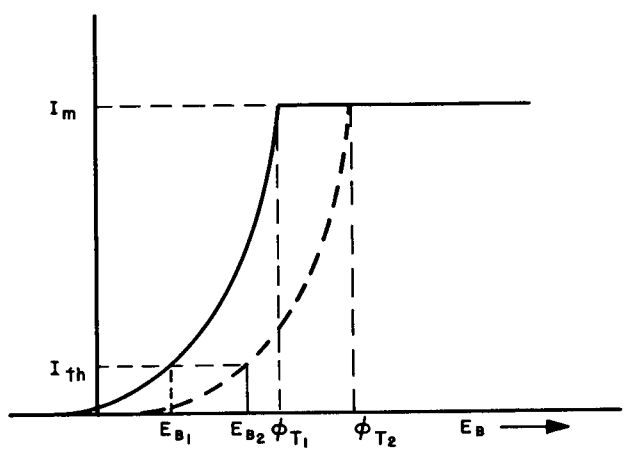

Fig. 3 - Plot of I vs E_B on two areas with different work functions for incident electrons having a half-Maxwellian energy distribution

In passing from the cathode to the target the electron beam is subject to the action of radial electric fields* at the apertures in G_1, G_2, and G_3 (Fig. 1). These fields increase the spread in velocities normal to the target. Also, because of incomplete space-charge

*The geometry of the experimental tube is cylindrical; therefore, the only electric fields are axial and radial. The axial fields do not perturb the distribution of velocities in the axial direction.

limiting, variations in the w.f., and geometrical nonuniformities on the surface of the cathode, the barrier ϕ_C which the electrons see at the cathode is not the same for all electrons in the beam. However, even though the velocity distribution has been changed, the beam as it approaches the target has the same distribution of velocities normal to the target regardless of what part of the target surface the beam is incident upon.* This means that the I vs E_B curves for any point on the surface will be the same, if the fields due to patches on the target surface do not deflect the electrons. In order to prevent patch fields from influencing the beam, a large electric field normal to the surface must be maintained. For a patch of diameter d that differs in w.f. from its surrounding by an amount $\Delta\phi$, the field F required to overcome the patch fields (3a) is roughly

$$F > \frac{\Delta\phi}{d} . \tag{2}$$

Under this condition the tangential electric fields due to differences in w.f. between patches are small, except in a limited region near the patch boundaries, thereby eliminating to a large degree the influence of the surrounding patches.

Even though the inequality in Eq. (2) might hold for all patches on the surface whose diameters are greater than or equal to the electron-beam diameter, there is another constraint which will affect the current received by any given point on the surface. Due to the presence of "micropatches" of diameter smaller than the beam diameter, the shape of the I vs E_B curve will differ slightly from one point to another on the surface. However, it can be shown that, if the distribution of velocities in the beam just outside of the patch-field region in front of the surface is Maxwellian in the high-velocity region, then for $E_B << \phi_T$ the $\log I$ vs E_B plot will be linear.

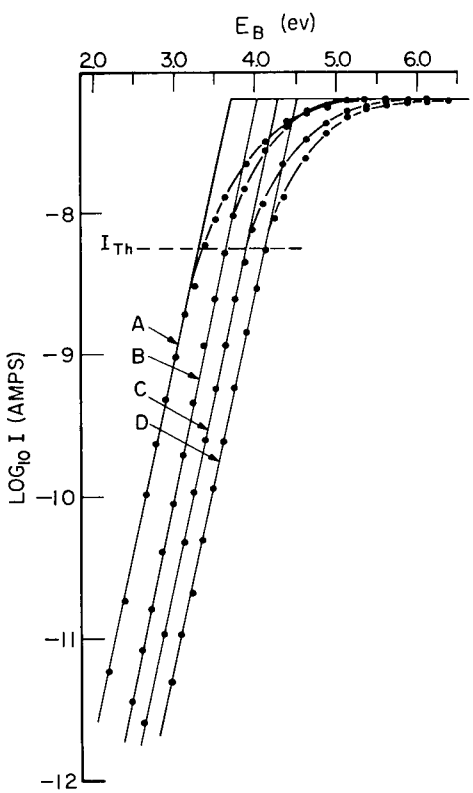

Fig. 4 - $\text{Log}_{10}\ I$ vs E_B for four different points on a uranium carbide target

In practice it is generally found that if the I vs E_B curves are taken sufficiently deep in the retarding-field region, the shape of the curves for two different areas covered by the beam is identical, but the curves are shifted with respect to each other on the energy axis by an amount $\bar{\bar{\phi}}_{T_1} - \bar{\bar{\phi}}_{T_2}$, where the $\bar{\bar{\phi}}_T$'s are a particular kind of average w.f. for each area (3b). In general $\bar{\bar{\phi}}$ is not the area average for the micropatches, but is determined by how much the external field F has exceeded the micropatch fields.

The curves of Fig. 4† are plots of $\log I$ vs E_B taken by stopping the electron beam on four separate points (A, B, C, and D) of a uranium carbide target. The points are marked on the kinescope pictures of the target presented in Fig. 5.† It is seen from the curves of Fig. 4 that there is a value of current I_{th} below which all the curves are linear. For $I < I_{th}$ any two

*Approximate calculations show that magnetic deflection of the type used here causes a negligible loss in forward energy due to deflection.

†Taken from Ref. 1

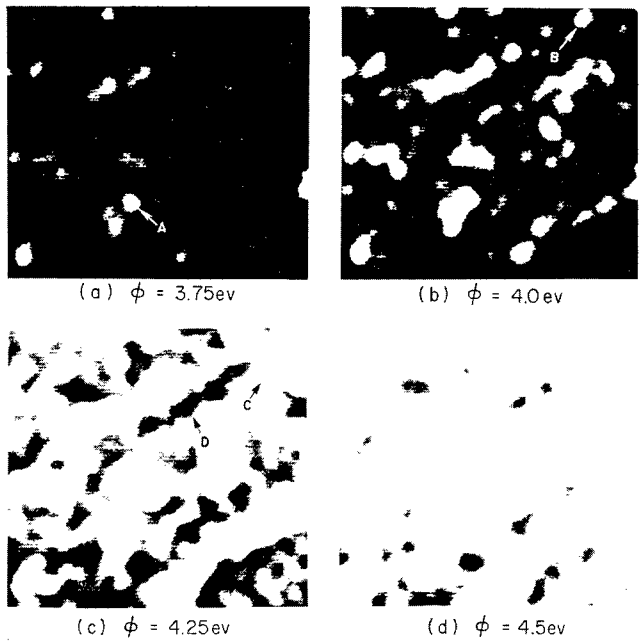

Fig. 5 - Kinescope images of a portion of a uranium carbide target at different beam energies

curves could be superimposed by shifting their abscissa by an amount equal to their contact potential difference.

EXPERIMENTAL TUBE

The experimental tube (Fig. 6) is very similar in physical structure and electron optical characteristics to the standard vidicon television camera tube. An electron beam of approximately 6 to 8 microns diameter (beam diameter varies slightly from tube to tube, depending on the size of the aperture in G_3) is obtained from the gun of the tube. Upon entering the drift space the beam is magnetically deflected. The deflection coils are of the standard vidicon type.

A 1000-mesh nickel screen having 40-percent transparency is mounted parallel to and about 0.2 cm in front of the target. The screen serves to maintain a high electric field normal to the target and prevents tangential patch fields on the target from changing the direction of the electron beam as it is incident on the target.

Focusing of the beam is done by imaging the 6 to 8 micron aperture in G_3 on the target by means of an axial magnetic field which is approximately constant over the length of the drift space. The combination of the deflecting and focusing field tends to make electrons spiral around the resultant magnetic-field lines, thus bringing the beam back parallel to the axis of the tube after it has been deflected.

The source of electrons in the beam is an oxide cathode (C in Fig. 1). The cathode is operated with a positive voltage of about 10 volts on G_1 and 500 volts on G_2, while G_3 is normally at 800 volts. Under these conditions some focusing of the electron beam onto G_3 takes place. The focusing is necessary in order to obtain enough current density on the 6-to-8-micron limiting aperture to give a usable beam current. This focusing,

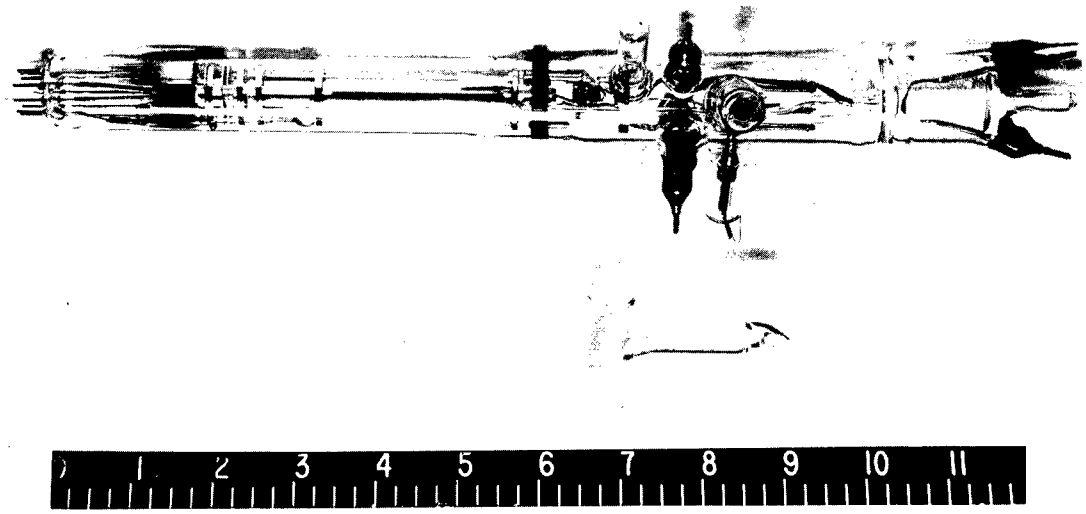

Fig. 6 - E.B.S. tube. The oxide cathode of the electron gun is on the left end. Near the right end are the target, target heater, tungsten ribbon, and target thermocouple feedthroughs. At the extreme right is a cesium getter used to provide a partial pressure of cesium for adsorption studies

however, has the undesirable effect of increasing the spread of the distribution of axial velocities in the beam. The effects of a large spread in beam velocity are discussed later.

Figure 7 shows a typical target assembly used in the experimental tube. The circular area in the center is the surface of the specimen to be examined. Stretched across the target assembly in the same plane as the specimen is a $0.001 \times 0.080 \times 0.500$ in. polycrystalline tungsten reference ribbon. The ribbon is supported in such a manner that it can be heated directly by passing current through it. The surface of the specimen is mounted on the end of a cylinder, inside of which is a tungsten filament capable of heating the specimen surface indirectly to temperatures of approximately 1400°C. The assembly picture in Fig. 7 contains a uranium carbide specimen. The exact design of the structure may differ slightly from one tube to another, depending upon the type of surface being investigated.

Fig. 7 - Target assembly with uranium carbide specimen

DISPLAY SYSTEM

To obtain an enlarged image, or pattern, of the w.f. variation on the surface being studied, the electron beam of a ten-inch-diameter kinescope is deflected with the same

scanning pattern as applied to the experimental tube being studied. The voltage drop developed across R_1 (Fig. 1) is amplified and used to drive the intensity grid of the kinescope. The signal is first ac amplified, dc restored, and then dc amplified to bring the signal to the level required for the desired contrast on the kinescope. The signal polarity is such that areas receiving higher currents (low w.f.) are brighter than areas receiving lower currents (high w.f.). The bias on the kinescope grid is adjusted so that the black level corresponds approximately to zero current through R_1. By proper adjustment of the amplification, the transition of an area from the black to white region on the kinescope can be made to occur in the region of beam current corresponding roughly* to I_{th}. Hence, if E_B is in the retarding-field region for some areas of the target, the light area of the kinescope face will correspond approximately to the area of the target having w.f. less than some value ϕ. The value of ϕ can be determined if a surface of known w.f. is scanned simultaneously with the surface being investigated (i.e., the tungsten ribbon shown in Fig. 7). The ribbon surface can be outgassed by passing current through it. Thus the w.f. of the specimen is compared with that of clean polycrystalline tungsten, which is usually about 4.5 ev. The pictures of Fig. 5† are the kinescope images of a uranium carbide target at room temperature for various values of E_B corresponding to the values of ϕ indicated below each picture. For example, from Fig. 5c it is seen that a little more than half the surface has a w.f. less than 4.25 ev.

METHODS OF OBTAINING PATCH DISTRIBUTION

Estimates of w.f. obtained from the kinescope images are not accurate enough to be of much use in constructing a patch-distribution curve. Greatly improved data are obtained by taking a large number of retarding-field plots, each at a different point on the surface.‡ The electronics of this system has been developed to take these retarding-field plots automatically. When a patch distribution is desired, the mode of scanning the surface is changed from one of continuous motion of the beam across the surface to one in which the beam is stepped from one point to another. The stepping is accomplished by making the current waveform through the fast-sweep deflection coils a stair-step waveform (Fig. 8). On the flat part of the waveform the beam is approximately stationary. During this dwell time the beam energy E_B is increased linearly with time by applying a negative-going sawtooth voltage to the cathode of the E.B.S. tube. The value of E_B from which the sawtooth starts is chosen lower than that required to obtain the current I_{th} from any point on the target. When the beam current I_{th} is reached, a threshold circuit (Fig. 1) is triggered, generating a trigger pulse. The trigger pulse turns off the cathode sawtooth, returning the cathode voltage to its initial value. The time τ at which the trigger occurs, with respect to the beginning of the sawtooth, is proportional to the beam energy required to obtain threshold current and is therefore a measure of the w.f. of the point being probed.

After the threshold has been triggered, no other sawtooth is started until the beam has moved to the next point on the target. The dwell time at any point is 100 microseconds, and about 12 microseconds are allowed for the beam to move to another point. This twelve microseconds is a minimum time determined by requirements to be discussed later. During each fast-sweep period 50 points are probed, and there are 600 fast-sweep lines in one complete scan of the surface, giving 30,000 separate points probed in one

*The transition from the black level to visible white on the kinescope does not occur at a sharp threshold of grid voltage, but over a small range of voltage, about 1/2 volt out of a total voltage of 25 volts for maximum signal.

†Taken from Ref. 1

‡The method of obtaining "patch" distributions described in this report differs from that described in Ref. 1. The principal drawbacks to the previous technique were the time required to plot a distribution curve and the fact that the average energy of the electron beam used in obtaining a distribution curve was high enough to cause appreciable desorption of active layers from some surfaces.

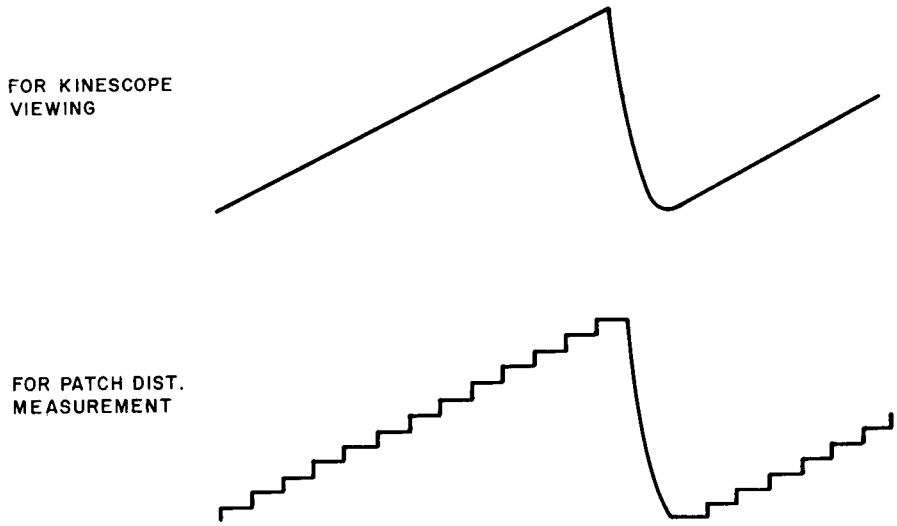

Fig. 8 - Current waveform through fast-sweep deflection coils of the electron-beam scanning tube

scan of the surface. It is seen that if the total area being scanned is less than 600 beam diameters on a side there will be some overlapping.

Each of the 30,000 threshold pulses is analyzed by an RIDL 400-channel analyzer* and stored in a channel corresponding to the w.f. it represents. The analyzer has a magnetic-core memory of 400 channels, and each channel has a storage capacity of 10^5 samples. The channel number in which a sample is stored is proportional to τ, which is in turn proportional to the w.f.

No internal modifications of the analyzer are required. Only two externally generated pulses (having the proper time relationships) are needed. One pulse is a gating pulse, which is turned on when the cathode sawtooth begins and turned off when the threshold circuit is triggered. During the time this gate is applied, an 8 Mc/sec oscillator in the analyzer is allowed to run. Every other pulse out of the oscillator is counted, and the channel number in which storage will take place is one-half the number of cycles generated by the oscillator (minus the first 20 cycles, which do not advance the channel count). After the oscillator is turned off by the gate, a unit count is stored automatically in the channel number to which the oscillator has counted. Twelve microseconds must be allowed for the storage operation to take place. After 12 microseconds an external "reset" pulse is applied, so that the channel-number count will start from zero when the 8-Mc oscillator is next turned on. The cathode sawtooth is generally adjusted so that the time required to store a count in channel 400 corresponds to a beam energy change of four volts. Consequently the w.f. difference between channels is 0.010 volts. This w.f. difference can be made smaller or larger by adjusting the total voltage swing of the cathode sawtooth. The lengths and time relationships of the pulses described are shown in Fig. 9.

The analyzer provides a visual display on an oscilloscope tube of the curve representing the number of sampled points on the surface having w.f. between ϕ and $\phi + \Delta\phi$ ($\Delta\phi \simeq 0.010$ volts) plotted against ϕ. This curve can be automatically plotted on an X-Y

*The analyzer is made by Radiation Instrument Development Laboratory, Melrose Park, Ill.

UNCLASSIFIED

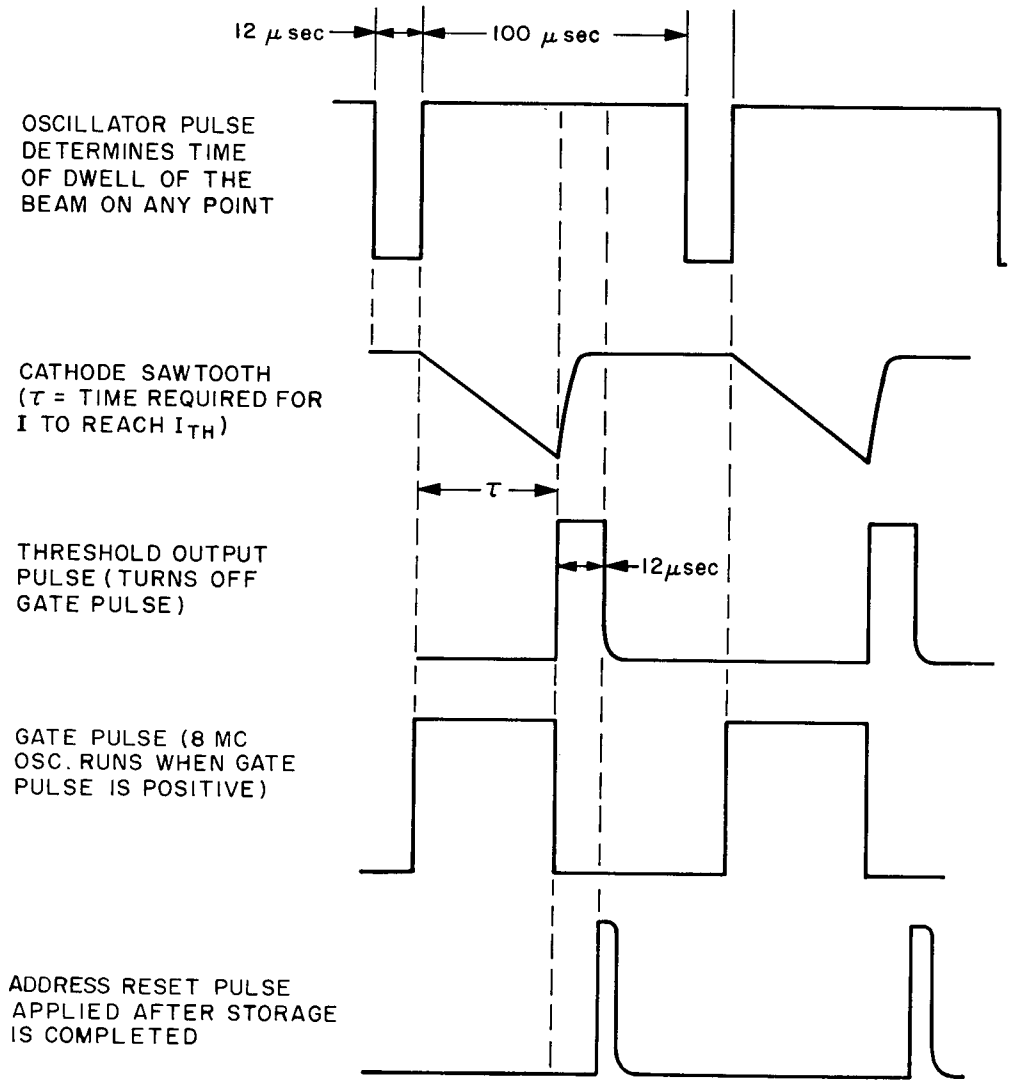

Fig. 9 - Time relationships of control pulses

recorder. A representative curve is shown in Fig. 10. The distribution centered about the w.f. of 2.65 ev was taken on a 0.03 cm^2 area of a barium-nickel matrix cathode which was in a state of incomplete activation. The target temperature was 773°K. The narrow distribution centered about 4.5 ev was taken on a polycrystalline tungsten ribbon mounted adjacent to the nickel matrix cathode. The inset photograph is the kinescope image of a smaller area (7×10^{-4} cm^2) of the same nickel matrix cathode with V_c at 1 ev.

The peak-to-peak magnitude of the current applied to both the fast-sweep and slow-sweep deflection coils can be varied independently from zero to the current required to scan one centimeter on the target assembly. This control allows one to scan and take samples on an area of the target surface of any desired size. The average dc level of the deflection current can also be varied independently, giving the option of selecting any spot on the target as a center about which to scan. By making the time-varying component of the deflection current zero in each coil, the beam can be stopped at any point on the surface. By reducing one (either fast or slow) of the deflection currents to zero, a line of any length can be scanned.

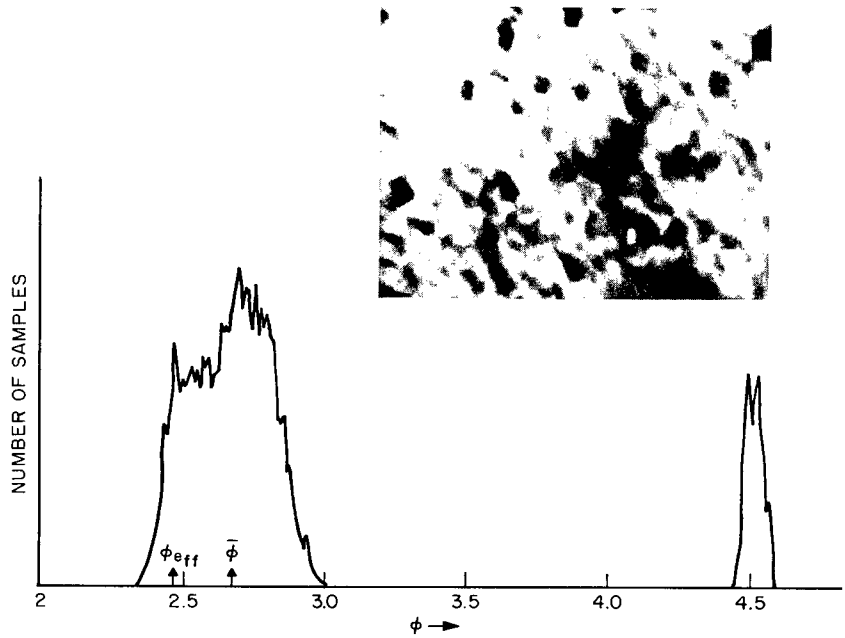

Fig. 10 - Work-function distribution of barium-nickel matrix cathode and tungsten ribbon. The quantity ϕ_{eff} is the work function obtained from thermionic emission measurements; $\bar{\phi}$ is the area average work function

MEASUREMENT ERRORS AND LIMITATIONS

The smallest difference in w.f. that can be resolved is dependent on both the spread in the axial-velocity distribution of the electron beam, the ratio of the maximum beam current to noise currents, and other extraneous voltages that might be present on the video signal after it is amplified.

To get an estimate of these effects on the w.f. measurements, we observe from Fig. 4 and the previous discussion that in the region of beam current where $I \leq I_{th}$, the experimental retarding-field curve is approximately of the form,

$$I = C \exp\left[E_B/kT_e\right] \tag{3}$$

where C is a constant for a given point on the surface, E_B is the electron-beam energy, and T_e is the electron-beam temperature. The temperature is obtained from the slope of the retarding-field plots at values of $I < I_{th}$ and is given by

$$kT_e = \left(2.303 \frac{\partial}{\partial E_B} \log_{10} I\right)^{-1}. \tag{4}$$

From Eq. (3) it is seen that for a small noise current ΔI, where $\Delta I << I_{th}$, the error in the value of E_B at which the threshold circuit triggers is given by

$$\Delta E_B = kT_e \frac{\Delta I}{I_{th}} = \delta\phi = \text{w.f. error}. \tag{5}$$

The noise present on the video signal is usually dominated by the thermal noise generated in the resistor R_1. The rms value of this noise current is given by

$$\Delta I_{rms} = \left(\frac{4kT\Delta f}{R_1}\right)^{1/2}, \tag{6}$$

in which T is the resistor temperature (°K), R_1 is the resistance (ohms), and Δf is the bandpass of the amplifier (cycles/sec). Such random noise has a Gaussian distribution in amplitude with a half width of 2.36 ΔI_{rms}. Consequently, for many samples of a point having w.f. ϕ one should obtain a Gaussian distribution about ϕ having a half width

$$\delta\phi_h = kT_e \frac{(2.36)\ \Delta I_{rms}}{I_{th}}. \tag{7}$$

The value of R_1 is 3.3×10^4 ohms, and the amplifier bandpass is approximately 2×10^5 cps. At room temperature these values give an rms noise current of 3.2×10^{-10} amperes. From the curves of Fig. 4 $kT_e \simeq 0.18$ ev, and $I_{th} = 5\times10^{-9}$ amperes. Using the above values in Eq. (7), a half-width of 0.026 ev is obtained for the error due to thermal noise.

It is seen from Eq. (7) that the uncertainty in w.f. due to noise currents increases with kT_e and $\Delta I(\text{noise})/I_{th}$. The focusing action at the apertures G_1, G_2, and G_3 through which the beam must pass increases the spread in the energy distribution of the beam, thereby increasing T_e and decreasing the value of I that can be used for I_{th}. From this standpoint it is desirable to choose the operating voltages for the experimental tube so as to produce a minimum of focusing action at the apertures. However, in desiring to improve the spatial (or image) resolution of the system, limiting apertures of eight microns or less are used in G_3, and in order to obtain an adequate beam current some focusing of the beam onto G_3 is necessary. The amount of focusing that can be used is limited by the spread in beam energy that can be tolerated. In practice the G_1 and G_2 voltages are adjusted for an optimum between T_e and I_{th}.

Figure 11 is a curve obtained by probing two adjacent spots (approximately ten microns apart) on the surface of a stainless steel target whose work functions differ by 0.050 ev. Each spot had its w.f. sampled 13,500 times. The half-width of each peak is a

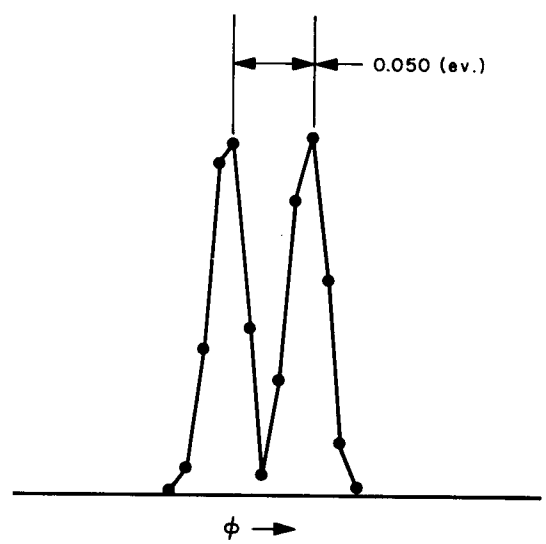

Fig. 11 - Work-function resolution illustrated by sampling work function on two adjacent points 0.050 ev apart (dots indicate the discrete channels 0.010 ev apart)

measure of the error due to noise. The almost Gaussian shape of the curves is consistent with the assumption that amplitude distribution of the noise currents is Gaussian. In this tube G_3 had a seven-micron aperture, kT_e was 0.22 ev, and I_{th} was 3×10^{-9} amperes. Resistor R_1 was cooled to 90°K with liquid nitrogen, thereby reducing the noise current by a factor of 0.56 from its room-temperature value. The above values in Eq. (7) give a half-width of 0.031 ev, which agrees well with the half-widths of the curves of Fig. 11. It is obvious from Fig. 11 that a w.f. resolution of 0.025 ev is possible with this tube.

The smallest patch diameter* that can be resolved (and consequently the amount of detail that can be seen in the kinescope image) is approximately equal to the electron-beam diameter. From the considerations outlined above, however, it is seen that there is a practical limit (determined by the desired w.f. resolution through Eq. (7)) to how small the beam diameter can be made through the use of a limiting aperture.

Another possible cause of error in the w.f. measurements is geometrical irregularity on the specimen surface. Irregularities such as grooves, holes, and others produce tangential electric fields that can deflect the electrons in the beam, and the stronger the applied field the greater those tangential fields become. Qualitatively (if tangential velocities are neglected) one expects that a groove or similar irregularity should appear to have higher w.f. than the surrounding area (provided the surroundings have the same w.f. as the actual w.f. of the groove surface). Many surfaces to be examined can be made flat to within a micron by polishing. However, some surfaces, e.g., oxide and matrix cathodes, cannot be polished. Consequently, for these surfaces one expects to have larger irregularities. Nonetheless, since most surfaces that have been observed thus far have relatively narrow spreads in w.f. when well cleaned or activated, it is believed that geometrical defects contribute very little to the measured spread in the w.f. distribution. Numerical calculations are now being made to determine the effect of simple types of irregularities.

Other potential contributions to the uncertainty in the measured w.f.'s are changes in the amplifier gain, cathode sawtooth nonlinearity, drift in the dc voltages on the cathode and G_1, and drift in the voltage level at which the threshold circuit triggers. Included with the long-term drift effects should be changes in the state of activation of the cathode in the E.B.S. tube and slow changes in the state of activation of the scanned surface. A rigorous examination of the circuits has established that errors in w.f. due to these effects are less than 0.005 ev. The long-term effects are minimized by being able to take a complete patch-distribution curve in approximately three seconds.

On some surfaces the electron beam could cause desorption of an active layer on the surface of the target, thus changing the w.f. while samples are being taken. Also, if the surface is at a low temperature there might be some charging of the surface by the beam due to poor conduction. Both these effects are minimized by terminating the cathode sawtooth in the deep retarding region (i.e., when the beam current reaches I_{th}).

The absolute value of w.f. of a specimen as determined by comparison with a clean polycrystalline tungsten ribbon† can also be verified by heating the surface to a sufficiently high temperature and measuring the thermionic electron current emitted by it. The current is measured by disconnecting R_1 and the ac amplifier and inserting a Keithley 600 electrometer in place of R_1. The effective w.f. ϕ_{eff} is obtained from the Richardson equation:

*On some tubes detail in the kinescope image as small as three microns has been observed. The beam diameter is roughly defined by the size of the limiting aperture in G_3. This aperture is drilled through a 0.001-in.-thick copper foil with a 0.0003-in. drill, and there can be imperfections in the hole resulting in variations in the effective beam diameter.

†Thermionic-emission measurements on tungsten ribbon from the same stock as the ribbon used in the experimental tube give an effective w.f. of 4.5 ± 0.05 ev for the reference ribbon.

$$J = AT^2 \exp\left[-\phi_{eff}/kT\right] \tag{8}$$

where

T = target temperature (°K),

$A \equiv 120$, and

J = measured emission current density.

With the field of 4000 volts/cm applied to the surface, one expects that all patches of diameter larger than the beam diameter should give thermionic emission independent of the w.f. of its surroundings. In this case the effective w.f. for the entire surface should be given by*

$$\phi_{eff} = \bar{\phi} - (0.30\ \Delta\phi_h)^2/kT \tag{9}$$

where $\bar{\phi}$ is the area average w.f., and $\Delta\phi_h$ is the half-width of a Gaussian distribution that can be fitted to the measured area distribution of w.f. For the distribution of Fig. 10 the experimental value obtained for ϕ_{eff} at $T = 773$°K is indicated on the patch distribution and lies roughly 0.19 ev below the area average w.f. Using $\Delta\phi_h \simeq 0.4$ ev in Eq. (9), the theoretical ϕ_{eff} falls 0.22 ev below the area average. Considering that the w.f.'s being compared were obtained by two entirely different techniques, one might consider this close agreement almost fortuitous.

With the provisions described for indirectly heating the target, it is possible to scan the surface and take patch distributions at different target temperatures. However, for low w.f. surfaces there will be an upper limit to the temperature that can be safely used. This limit is determined by the amount of power that the 1000-mesh screen will dissipate without damage (approximately 500 milliwatts). Using 800 volts on G_4 will then limit the thermionic-emission current from the target to about 6×10^{-4} amperes. The E.B.S. technique therefore provides a means of measuring the temperature dependence of the work function from very low temperatures to temperatures at which significant thermionic emission is obtained.

The 800 volts on G_4 could be lowered and the same field at the target surface could still be maintained if the spacing between target and screen is reduced. But it has been found that if the spacing is too close, the 1000-mesh screen will be imaged onto the target surface when the magnetic focusing field is adjusted to obtain the best target detail in the kinescope image.

SUMMARY

The E.B.S. technique provides a method of measuring the distribution of w.f. as well as the absolute value of w.f. on surfaces having sufficiently high surface conductivity. The absolute value of w.f. may be determined by two independent methods: by measuring the contact potential between the tungsten reference ribbon and the specimen surface, and by measuring the thermionic emission from the specimen.

Along with measuring the w.f. distribution and the absolute w.f., the E.B.S. technique offers a visual pattern of the distribution of the surface area in w.f., showing detail as small as three microns. The pattern shows the relative sizes and shapes of the various

*See Eqs. A2 and A3 of Ref. 1. Due to a typographical error overlooked during proofreading, the "plus" sign in Eq. A3 should read "minus."

"single" w.f. domains. By having independent control of the magnitude and centering of the beam scan in the X and Y directions, one can choose any arbitrary rectangular area of the surface to be analyzed.

Because the w.f. measurements are based on a contact potential difference method, measurements can be made from room temperature (or even below) to temperatures limited only by the power dissipation due to thermionic emission to the screen in G_4. Consequently, one can study low-temperature activation phenomena on practical thermionic emitters (having flat surfaces), e.g., oxide cathodes. Measurements of the temperature coefficient of w.f. may also be made over a larger range and at lower temperatures than are possible using the conventional thermionic-emission technique.

Resolution of w.f. differences of approximately 0.025 ev are obtained. The main limitations on the resolution in the measured w.f. are the signal-to-noise ratio of the amplifier system, and the velocity spread in the electron beam. Uncertainties in the w.f. caused by slow changes in the state of the surface, drift in the electronic circuitry, charging, and desorption effects are all minimized by taking enough samples (30,000) of w.f. for a statistical distribution in about 3.0 seconds, and by not allowing the beam current to exceed I_{th}.

In addition to its obvious use in studying thermionic-emitter surfaces, the E.B.S. system is well suited for studies of surface diffusion. By using a localized source of material, the diffusion rates and their temperature dependence can be measured for a wide variety of diffusing substances on various surfaces. Surface-adsorption studies can also be made by allowing a partial pressure (less than 10^{-6} mm Hg) of the gas of interest to be leaked into the tube, provided that the gas introduced does not poison the oxide cathode used in the electron gun. (The tube design is ideally suited for differential pumping, since the cathode end can be isolated from the target end by the eight-micron aperture in G_3.) Some limited adsorption studies have been made for cesium on tungsten, but as yet no diffusion experiments have been attempted.

REFERENCES

1. Haas, G. A., and Thomas, R. E., J. Appl. Phys. 34(12):3457 (1963)

2. Anderson, P. A., Phys. Rev. 47:958 (1935)

3. Herring, C., and Nichols, M. H., Rev. Mod. Phys. 21(2) (1949)

   a. p. 204
   b. p. 216

Security Classification

DOCUMENT CONTROL DATA - R&D

(Security classification of title, body of abstract and indexing annotation must be entered when the overall report is classified)

1. ORIGINATING ACTIVITY *(Corporate author)* U.S. Naval Research Laboratory Washington, D.C. 20390	2a. REPORT SECURITY CLASSIFICATION Unclassified 2b. GROUP --

3. REPORT TITLE

PRINCIPLES AND INSTRUMENTATION FOR THE MEASUREMENT OF WORK-FUNCTION VARIATIONS BY ELECTRON-BEAM SCANNING

4. DESCRIPTIVE NOTES *(Type of report and inclusive dates)*

An interim report on one phase of the problem.

5. AUTHOR(S) *(Last name, first name, initial)*

Thomas, Richard E., Haas, George A., and Harris, Franklin H.

6. REPORT DATE December 16, 1965	7a. TOTAL NO. OF PAGES 18	7b. NO. OF REFS 3
8a. CONTRACT OR GRANT NO. NRL Problem R08-05 b. PROJECT NO. RR 008-03-46-5652 c. d.	9a. ORIGINATOR'S REPORT NUMBER(S) NRL Report 6336 9b. OTHER REPORT NO(S) *(Any other numbers that may be assigned this report)*	

10. AVAILABILITY/LIMITATION NOTICES

Unlimited availability. Copies available from CFSTI - $1.00

11. SUPPLEMENTARY NOTES	12. SPONSORING MILITARY ACTIVITY Department of the Navy (Office of Naval Research)

13. ABSTRACT

An experimental tube and associated circuitry have been developed to measure the point-by-point variation (or "patchiness") in the work function of conductive surfaces. The technique involves scanning the surface with a small-diameter, low-energy electron beam in a television-like fashion. An enlarged image showing the pattern of the work-function variation on the surface is obtained on a kinescope tube. The associated circuitry also provides a method of obtaining, during one scan, the values of the work functions of many small regions of the scanned surface. These individual values are automatically catalogued and stored by means of a 400-channel analyzer which gives a plot of the area distribution in work function in about three seconds.

The minimum work-function "patch" size that can be resolved is determined approximately by the size of the electron beam (work-function variations with dimensions as small as three microns have been observed). In measuring "patch" distributions the system is capable of resolving differences in work function as small as 0.025 ev. This instrumentation was primarily designed for the purpose of measuring patch distributions on surfaces that might be used as thermionic sources of electrons in vacuum tubes and energy converters. However, since measurements may be made over a wide range of surface temperatures, other surface phenomena, e.g., adsorption and surface migration, may also be studied using this equipment.

DD FORM 1 JAN 64 1473

Security Classification

Security Classification

14. KEY WORDS	LINK A ROLE	LINK A WT	LINK B ROLE	LINK B WT	LINK C ROLE	LINK C WT
Electron beams						
Scanning						
Work functions						
Conductive surfaces						
Surface properties						
"Patch" distributions						

INSTRUCTIONS

1. ORIGINATING ACTIVITY: Enter the name and address of the contractor, subcontractor, grantee, Department of Defense activity or other organization *(corporate author)* issuing the report.

2*a*. REPORT SECURITY CLASSIFICATION: Enter the overall security classification of the report. Indicate whether "Restricted Data" is included. Marking is to be in accordance with appropriate security regulations.

2*b*. GROUP: Automatic downgrading is specified in DoD Directive 5200.10 and Armed Forces Industrial Manual. Enter the group number. Also, when applicable, show that optional markings have been used for Group 3 and Group 4 as authorized.

3. REPORT TITLE: Enter the complete report title in all capital letters. Titles in all cases should be unclassified. If a meaningful title cannot be selected without classification, show title classification in all capitals in parenthesis immediately following the title.

4. DESCRIPTIVE NOTES: If appropriate, enter the type of report, e.g., interim, progress, summary, annual, or final. Give the inclusive dates when a specific reporting period is covered.

5. AUTHOR(S): Enter the name(s) of author(s) as shown on or in the report. Enter last name, first name, middle initial. If military, show rank and branch of service. The name of the principal author is an absolute minimum requirement.

6. REPORT DATE: Enter the date of the report as day, month, year; or month, year. If more than one date appears on the report, use date of publication.

7*a*. TOTAL NUMBER OF PAGES: The total page count should follow normal pagination procedures, i.e., enter the number of pages containing information.

7*b*. NUMBER OF REFERENCES: Enter the total number of references cited in the report.

8*a*. CONTRACT OR GRANT NUMBER: If appropriate, enter the applicable number of the contract or grant under which the report was written.

8*b*, 8*c*, & 8*d*. PROJECT NUMBER: Enter the appropriate military department identification, such as project number, subproject number, system numbers, task number, etc.

9*a*. ORIGINATOR'S REPORT NUMBER(S): Enter the official report number by which the document will be identified and controlled by the originating activity. This number must be unique to this report.

9*b*. OTHER REPORT NUMBER(S): If the report has been assigned any other report numbers *(either by the originator or by the sponsor)*, also enter this number(s).

10. AVAILABILITY/LIMITATION NOTICES: Enter any limitations on further dissemination of the report, other than those imposed by security classification, using standard statements such as:

(1) "Qualified requesters may obtain copies of this report from DDC."

(2) "Foreign announcement and dissemination of this report by DDC is not authorized."

(3) "U. S. Government agencies may obtain copies of this report directly from DDC. Other qualified DDC users shall request through _____."

(4) "U. S. military agencies may obtain copies of this report directly from DDC. Other qualified users shall request through _____."

(5) "All distribution of this report is controlled. Qualified DDC users shall request through _____."

If the report has been furnished to the Office of Technical Services, Department of Commerce, for sale to the public, indicate this fact and enter the price, if known.

11. SUPPLEMENTARY NOTES: Use for additional explanatory notes.

12. SPONSORING MILITARY ACTIVITY: Enter the name of the departmental project office or laboratory sponsoring *(paying for)* the research and development. Include address.

13. ABSTRACT: Enter an abstract giving a brief and factual summary of the document indicative of the report, even though it may also appear elsewhere in the body of the technical report. If additional space is required, a continuation sheet shall be attached.

It is highly desirable that the abstract of classified reports be unclassified. Each paragraph of the abstract shall end with an indication of the military security classification of the information in the paragraph, represented as *(TS)*, *(S)*, *(C)*, or *(U)*.

There is no limitation on the length of the abstract. However, the suggested length is from 150 to 225 words.

14. KEY WORDS: Key words are technically meaningful terms or short phrases that characterize a report and may be used as index entries for cataloging the report. Key words must be selected so that no security classification is required. Identifiers, such as equipment model designation, trade name, military project code name, geographic location, may be used as key words but will be followed by an indication of technical context. The assignment of links, roles, and weights is optional.